Submitted to Physics of Plasmas

Probabilistic finite-size transport models for fusion: anomalous transport and scaling laws

B.Ph. van Milligen

Asociación EURATOM-CIEMAT para Fusión,

Avda. Complutense 22, 28040 Madrid, Spain

R. Sánchez

Departamento de Física, Universidad Carlos III,

Avda. de la Universidad 30, 28911 Leganés, Spain

B.A. Carreras

Fusion Energy Division, Oak Ridge National Laboratory,

P.O. Box 2001, Oak Ridge TN 37831-2001, USA

(Dated: January 29, 2004)

Abstract

Transport in fusion plasmas in the low confinement mode is characterized by several remarkable properties: the superdiffusive scaling of transport with system size, stiff (or "canonical") profiles, power degradation and rapid transport phenomena. The present paper explores the possibilities of constructing a unified transport model, based on the Continuous-Time Random Walk, in which all these phenomena are handled adequately. The resulting formalism appears to be sufficiently general to provide a sound starting point for the development of a full-blown plasma transport code, capable of incorporating the relevant microscopic transport mechanisms, and allowing predictions of confinement properties.

I. INTRODUCTION

Radial transport in the magnetic confinement devices used in thermonuclear fusion research has a strong stochastic component [1]. The motion of individual charged particles in these systems is affected by collisions, by the interaction with the magnetic field [2], and instabilities and turbulence [3, 4]. The magnetic field has a toroidal topology and is characterized by nested magnetic surfaces, embedded islands and stochastic zones [5–7]. Thus, it is not surprising that the macroscopic transport in this exceedingly complex system is not properly described by a classical diffusive equation, in which the transport properties of the system are modeled through a set of diffusivities and conductivities. The appropriateness of the diffusive (or "Fickian") approach ultimately relies on the existence of some microscopic scales that govern the transport in the system (for instance, the ion Larmor radius, the eddy size, the collision frequency or the eddy turnover time). If such characteristic scales exist, then the experimentally obtained diffusivities and conductivities can be used to predict transport in a system of a different (larger) size. However, most studies of global scaling properties of transport indicate that the transport parameters do depend on the system size [8]. This strongly suggests that transport in these devices lacks such a characteristic scale: the scales governing transport are only limited by the system size and the discharge duration. Perturbative experiments also point towards the absence of a characteristic scale, namely via the existence of so-called "long-range correlations" [9]. This state of things suggests that, to be able to describe plasma transport properly and make reliable extrapolations towards larger system sizes, it might be more appropriate to look for alternate descriptions to the Fickian approach that do not rely explicitly on the existence of such characteristic scales.

Several approaches to this problem have been explored in recent publications. A well-known generalization of diffusive transport is the Continuous Time Random Walk (CTRW) [10], in which the microscopic motion of individual particles is governed by certain probability distributions. When these probability distributions are chosen to be of the Lévy type, scale-free transport may result. One of the first examples of its use to study plasma transport in stochastic magnetic fields can be found in **Ref. 1**. The CTRW approach is closely connected to system descriptions in terms of Fractional Differential Equations (FDEs) [11–14], that has also been explored recently in the context of plasma trans-

port [15, 16]. An alternative and more qualitative approach to the problem was provided by the ideas of self-organized criticality (SOC) [17]. It was shown that "sandpile" toy models exhibit dynamics that are qualitatively similar to those encountered in a confined plasma, at least in terms of global confinement time scaling and rapid propagation phenomena [18–20]. It has however remained difficult to translate any of these related approaches into a useful transport model for fusion plasmas.

The work presented in this paper must be understood in this context. Our purpose is to explore the possibilities of CTRW models for describing transport in fusion plasmas and to identify the minimal ingredients needed to reproduce the basic phenomenology observed in the experiment. In particular, we focus our attention on the most important predictive tool in fusion research, namely the global confinement time τ (of particles or energy), and its scaling with the system size, the source rate P_{ext} (denominated "heating" or "power deposition" in the fusion context) and other global parameters. Experiments show that τ deteriorates with the external power source (as $\tau \sim P_{ext}^{-0.5-0.7}$) and that it scales slower than the diffusive prediction ($\tau \sim L^2$) with the system size [8]. In addition, we investigate the possibility of handling superdiffusive propagation of perturbations in the modelling framework, as this also is an important characteristic of transport in fusion plasmas.

The paper is organized as follows. In Section II the theory of CTRW's will be discussed, and we will pay particular attention to the possibility of modelling the CTRW system by means of a Master Equation (ME). The ME provides a **probabilistic** description of the CTRW, thus eliminating the need for constructing a particle tracking code, and greatly enhancing the practical usefulness of this approach. The ME is derived for a particular CTRW, not previously studied in literature, namely with explicit space- and time dependence of the particle step probability distribution function (pdf), for a finite-size system, and with an external source. These particular properties make this CTRW very appropriate for modelling transport in fusion plasmas. In Section III, a toy model based on these ideas is explored numerically to demonstrate that it indeed exhibits the desired phenomenology. Section IV provides a discussion and Section V gives some conclusions. In summary, it is suggested that the CTRW formalism might be a serious candidate to implement all these ideas in the framework of a unified model of transport in fusion plasmas with real predictive capabilities.

II. THEORY

The classical 1-dimensional Continuous-Time Random Walk (CTRW) model [10] consists of particles or walkers (we will use both terms interchangeably) that wait in their position x for a lapse of time Δt and then take a step of size Δx. Δt and Δx are drawn from a joint probability density function (pdf) ξ. Following the standard use in statistics, we reserve the name 'probability distribution' (PDF) for the probability of the walker performing a jump smaller than Δx after a lapse of time shorter than Δt; thus the pdf is the derivative of the PDF with respect to both arguments. This joint pdf then depends, in its most general form, on the space and time coordinates of both the origin and the destination of each particle jump: $\xi(x-x', x'; t-t', t')$ specifies the probability that the particle makes a jump of size $\Delta x = x - x'$, from x' to x, after having remained a time $\Delta t = t - t' \geq 0$ at x'. Conservation of probability requires that:

$$\int_{-\infty}^{\infty} dx \int_{0}^{\infty} d\tau \; \xi(x-x', x'; \Delta t, t') = 1, \quad \forall x', t'. \tag{1}$$

The system may exhibit a vast spectrum of dynamical behavior, depending on the form of the pdf ξ, that will result in different functional forms for the probability density of finding the walker in x at time t, $n(x,t)$. We will also refer to $n(x,t)$ as *particle density*, for if the motion of N walkers is given by the joint pdf, the number of particles at position x and time t is $N \cdot n(x,t)$. If we choose ξ to be a product of the form:

$$\xi(x-x', x'; \Delta t, t') = \frac{e^{(x-x')^2/4\sigma^2}}{2\sigma\sqrt{\pi}} \cdot \frac{e^{-\Delta t/\tau_D}}{\tau_D}, \tag{2}$$

the resulting CTRW is a diffusive process with diffusion coefficient $D = \sigma^2/\tau_D$ (cf. Appendix B).

As mentioned in the Introduction, it is useful that the CTRW model possesses an associated Master Equation. This requirement reduces the range of admissible choices for ξ somewhat. Here, we will assume that the pdf is *separable*:

$$\xi(x-x', x'; t-t', t) = p(x-x', x'; t)\psi(x'; t-t'). \tag{3}$$

This pdf is separable in the sense that ξ is the product of two statistically independent pdfs, namely p for the particle step-size and ψ for the waiting time. Note that we have intentionally

assumed that ψ is *invariant* in time, but at the same time we permit a dependence on (x', t) of p. It will soon become clear that this particular choice is sufficiently unrestrictive to permit interesting dynamics in the sense of the Introduction.

In the following subsections (II A - II E) we shall discuss some general properties of this particular CTRW model. First, in Section II A we will prove that a Master Equation indeed exists for the joint pdf defined by Eq. (3). Second, if the CTRW is to be able to describe transport in confined plasmas, it must be spatially restricted to a bounded domain and admit steady state solutions. These issues are discussed in Section II B. In Sections II C and II D we will discuss how the CTRW defined in Eq (3) must be modified to describe a transport model that lacks any characteristic scale and exhibits "power degradation" similar to that encountered in real plasmas. Finally, all these results are collected in Section II E, where a general form for a CTRW model encompassing all these properties is proposed.

A. The Master Equation

In this subsection, we intend to show that it is indeed possible to find a Master Equation that corresponds to the CTRW model defined by Eq. (3). This is a non-trivial exercise, due to the explicit time dependence in the step size pdf p, which is not usually considered in the literature on CTRW models [21]. Generally speaking, a Master Equation is an evolution equation for the local probability density of finding a walker at a given location at a given time [22]. In the infinite spatial domain, it has the general form:

$$\begin{aligned}\frac{\partial n(x,t)}{\partial t} &= \int_0^t dt' \int_{-\infty}^{\infty} dx' K(x', x-x'; t', t-t') n(x', t') \\ &- \int_0^t dt' n(x,t') \left[\int_{-\infty}^{\infty} dx' \; K(x, x'-x; t', t-t') \right], \end{aligned} \tag{4}$$

where the kernel $K(x', x-x'; t', t-t')$ gives the transition probability of finding at x at time t a particle that was at x' at time t'. The first term of the r.h.s. gives the contribution of particles arriving at x between times 0 and t, and the second term that of particles leaving x between times 0 and t. The kernel must guarantee particle conservation, so:

$$\int_0^{\infty} d\tau \int_{-\infty}^{\infty} dx \; K(x', x-x'; t', \tau) = 1. \tag{5}$$

The probability density that appears in the Master Equation is the ensemble average over many different realizations of the CTRW for a single walker. In this sense, it yields a **probabilistic** description of the evolution of a large number of walkers, having self-evident advantages from a computational point of view, since it eliminates the need to follow a large amount of particles simultaneously.

To derive an ME for the joint pdf defined in Eq. (3) we proceed initially by following **Ref. 21**. First, we write the probability of finding the walker at x at time t as:

$$n(x,t) = \int_0^t \eta(x; t-t')Q(x;t')dt', \tag{6}$$

where $\eta(x; t-t')$ represents the probability that a walker, located at x' at time t', remains in the same position at time t. Clearly, this probability is given by:

$$\eta(x';t) = 1 - \int_0^t d\tau\psi(x';\tau) \tag{7}$$

The quantity $Q(x;t)$ represents the total probability of the walker arriving at position x at time t by any possible route (any number of jumps) [23]. Thus, it can be decomposed as a sum over the probabilities of arriving there by a fixed number of jumps:

$$Q(x;t) = \sum_{j=0}^{\infty} Q^j(x;t) \tag{8}$$

where $Q^j(x;t)$ is the probability of arriving at position x at time t by precisely j jumps. By definition, $Q^j(x;t)$ satisfies the following recurrence relation:

$$Q^j(x;t) = \int_{-\infty}^{\infty} dx' \int_0^t dt'\xi(x-x', x'; t-t', t)Q^{j-1}(x';t') \tag{9}$$

with the initial condition

$$Q^0(x;t) = \delta(x)\delta(t), \tag{10}$$

which simply reflects the fact that the walker cannot move in a time interval of zero length.

Combining Eqs. (8), (9) and (10) yields a recursive equation for $Q(x;t)$:

$$Q(x;t) - \delta(x)\delta(t) = \int_{-\infty}^{\infty} dx' \int_0^t dt'\xi(x-x', x'; t-t', t)Q(x';t'), \tag{11}$$

which is the starting point in the derivation of the Master Equation. Inserting our choice of ξ, given by Eq. (3), we obtain:

$$Q(x;t) - \delta(x)\delta(t) = \int_{-\infty}^{\infty} dx' p(x-x',x';t) \int_0^t dt' \psi(x';t-t') Q(x';t') \tag{12}$$

At this point we must depart from the derivation made in **Ref. 21**, since our problem is not spatially invariant due to the explicit dependence of both p and ψ on x'. We can, however, use the Laplace transform:

$$L\left[f(t)\right] = f(s) = \int_0^{\infty} e^{-st} f(t) dt \tag{13}$$

to rewrite the convolution in Eq. (6) as:

$$n(x,s) = \eta(x;s) Q(x;s) \tag{14}$$

This, together with the auxiliary distribution

$$\phi(x;s) = \frac{\psi(x;s)}{\eta(x;s)} \tag{15}$$

allows us to rewrite the last integral in the r.h.s. of Eq. (12) as:

$$\begin{aligned} \int_0^t dt' \psi(x';t-t') Q(x';t') &= L\left[\psi(x';s) Q(x';s)\right] \\ = L\left[\phi(x';s) n(x',s)\right] &= \int_0^t dt' \phi(x';t-t') n(x',t') \end{aligned} \tag{16}$$

so that Eq. (12) becomes:

$$Q(x;t) - \delta(x)\delta(t) = \int_{-\infty}^{\infty} dx' p(x-x',x';t) \int_0^t dt' \phi(x';t-t') n(x',t') \tag{17}$$

Applying the Laplace transform to Eq. (17) we find:

$$Q(x;s) - \delta(x) = g(x;s), \tag{18}$$

where we have defined

$$g(x;s) = L\left[\int_{-\infty}^{\infty} dx' p(x-x',x';t) \int_0^t dt' \phi(x';t-t') n(x',t')\right]. \tag{19}$$

Multiplying Eq. (18) left and right by $s\eta(x;s)$ and using Eq. (14), it can be written:

$$[sn(x,s) - \delta(x)] - \delta(x)\,[s\eta(x;s) - 1] = (s\eta(x;s) + 1 - 1)g(x;s) \tag{20}$$

Using $L\,[\partial f/\partial t] = sf(s) - f(0)$, Eq. (20) can be Laplace-inverted to obtain:

$$\frac{\partial n(x,t)}{\partial t} = \delta(x)\frac{\partial \eta(x;t)}{\partial t} + \int_0^t dt' \int_{-\infty}^{\infty} dx' \phi(x';t-t')p(x-x',x';t)n(x',t') \\ + L^{-1}\left[(s\eta(x;s) - 1)g(x;s)\right] \tag{21}$$

To simplify the last term in Eq. (21), we again use Eq. (18):

$$g(x;s) = \frac{n(x,s)}{\eta(x;s)} - \delta(x), \tag{22}$$

which, combined with the Laplace transform of Eq. (7), allows us to write:

$$(s\eta(x;s) - 1)g(x;s) = -\phi(x;s)n(x,s) + \delta(x)\psi(x;s) \tag{23}$$

This result can be used to Laplace-invert the last term in the r.h.s. of Eq. (21), so that this equation becomes:

$$\frac{\partial n(x,t)}{\partial t} = \int_0^t dt' \int_{-\infty}^{\infty} dx' \phi(x';t-t')p(x-x',x';t)n(x',t') \\ - \int_0^t dt' \phi(x;t-t')n(x,t') \tag{24}$$

which is the Master Equation we sought. The transition kernel appearing in Eq. (4) is thus given by:

$$K(x', x-x'; t', t-t') = \phi(x';t-t')p(x-x',x';t). \tag{25}$$

B. Restricted CTRW: steady state

The CTRW must be spatially bounded to be useful for describing transport in confined plasmas. Without loss of generality, we will assume it to be restricted to the region $0 \leq x \leq 1$, i.e. x is a normalized spatial coordinate that absorbs the system size. When a particle takes a step such that its new position x lies outside of the range $[0,1]$, it is considered lost.

Thus, particles are no longer conserved inside the system, and an external source rate $S(x,t)$ must be included for the CTRW to yield steady state solutions. Note that the finite size and the continuous fueling set our model somewhat aside from some other general systems studied in the CTRW framework [21].

The ME that corresponds to the restricted CTRW differs slightly from Eq. (24). It is easy to see that the derivation of the previous subsection remains essentially unchanged if we assume that once the walker moves outside of $[0,1]$ it is lost. This is so because the only mathematical tool that was used in the derivation is the Laplace transform, to exploit the time-invariance of the unrestricted case, and this symmetry property is also present in the (spatially) restricted case. In fact, for the restricted CTRW, the equation equivalent to Eq. (24) is:

$$\frac{\partial n(x,t)}{\partial t} = \int_0^t dt' \int_0^1 dx' \phi(x';t-t') p(x-x',x';t) n(x',t') - \int_0^t dt' \phi(x;t-t') n(x,t'). \tag{26}$$

The only effect of restricting the CTRW is to modify the integration limits of the first term in the r.h.s., which accounts for the particles coming to x at time t from other locations in the spatial domain. However, this equation differs formally from a standard ME in a finite domain [22], since the spatial integral of the transition kernel in the second term of the r.h.s. extends over $[-\infty,\infty]$, not $[0,1]$ (see Eq. (4)) to account not only for the transfer of particles from x to other locations inside $[0,1]$, but also for direct transfer out of the system. However, it is possible to recover the standard ME form by rewriting it as:

$$\frac{\partial n(x,t)}{\partial t} = \int_0^t dt' \int_0^1 dx' \phi(x';t-t') p(x-x',x';t) n(x',t') - \int_0^t dt' \phi(x;t-t') n(x,t') \left[\int_0^1 dx' p(x'-x,x;t) \right] - L(x,t), \tag{27}$$

where $L(x,t)$ is given by:

$$L(x,t) = \int_0^t dt' \phi(x;t-t') n(x,t') \left[1 - \int_0^1 dx' p(x'-x,x;t) \right]. \tag{28}$$

Here, $L(x,t)$ is identified with particle losses through the system boundaries originating at position x at time t. Thus, this term may also be viewed as an absorbing boundary condition at the boundaries of the domain of the restricted CTRW.

As mentioned before, we include an external source $S(x,t)$ to balance these losses and allow the system to reach steady state. Thus, the final ME for the restricted CTRW reads:

$$\frac{\partial n(x,t)}{\partial t} = S(x,t) + \int_0^t dt' \int_0^1 dx' \phi(x';t-t') p(x-x',x';t) n(x',t') - \int_0^t dt' \phi(x;t-t') n(x,t'). \tag{29}$$

The system will possess a steady state **in the presence of a time-independent external source**, if the number of particles confined *inside any finite part of the system* is constant in time. **This condition can be rewritten as**:

$$S(x) = -\int_0^1 dx' n(x')\ p(x-x',x';t) \int_0^t dt' \phi(x';t-t') + n(x) \int_0^t dt' \phi(x;t-t'), \tag{30}$$

which requires that the r.h.s. of Eq. (30) must be independent of time. Thus, p and ψ cannot be both chosen arbitrarily, which is a subtle but important consequence of our choice for the joint pdf ξ (Eq. (3)). A particularly simple case is that in which the step size pdf p is time-independent. Then, to reach steady state it is sufficient that:

$$\phi(x';t-t') = g(x')\ \delta(t-t'), \tag{31}$$

i.e. the waiting time pdf must follow an exponential law:

$$\psi(x';t-t') = g(x') e^{-g(x')(t-t')}. \tag{32}$$

In the remainder of this paper, we will restrict the discussion to exponential waiting time distributions.

C. The absence of characteristic scales

In this section, we will briefly discuss the scaling properties of the CTRW model defined by Eq. (29). We will show that the model is general enough to include transport processes that are not dependent on the existence of any underlying characteristic scales. Central to this

discussion is the concept of "global confinement time" of the system, since the characteristic length scale issue was raised in relation with the (anomalous) scaling of this quantity with system size. For the CTRW it is defined as:

$$\tau = \frac{N_{tot}}{S_{tot}}, \tag{33}$$

where N_{tot} is the total particle content in steady state and S_{tot} is the total source rate, integrated over x, where $S(x,t)$ is assumed to be independent of time.

The existence of characteristic time and length scales is intrinsic to the classical diffusive random walk, defined by the joint pdf Eq. (2). Its associated ME is obtained by combining Eq. (2) with Eq. (29):

$$\frac{\partial n(x,t)}{\partial t} = S(x) + \frac{1}{\tau_D}\left[\frac{1}{2\sigma\sqrt{\pi}}\int_0^1 dx' n(x',t) e^{(x-x')^2/4\sigma^2} - n(x,t)\right] \tag{34}$$

Usually, diffusive transport is not described by this equation, but rather by:

$$\frac{\partial n}{\partial t} = \left(\frac{\sigma^2}{\tau_D}\right)\frac{\partial^2 n}{\partial x^2} + S(x), \tag{35}$$

which can readily be derived from Eq. (34) using a Taylor expansion of the density, since all moments of arbitrary order of p and ψ are finite, thanks to the exponential tails of the pdfs for large $(x - x')$ and τ. Significantly, all moments of p can be expressed in terms of its second moment,

$$\left\langle \Delta x^2 \right\rangle = \frac{1}{2\sigma\sqrt{\pi}}\int_{-\infty}^{\infty} d(\Delta x) \ \cdot (\Delta x)^2 \cdot e^{(\Delta x)^2/4\sigma^2} = 2\sigma^2. \tag{36}$$

For this reason, σ acts as a true characteristic length scale of the system: since σ is is usually much smaller than the system size (i.e., $\sigma << 1$), restricting the integration in Eq. (36) to the system domain $[0,1]$ still yields an estimation for $\langle \Delta x^2 \rangle$ which is essentially equal to $2\sigma^2$. This insensitivity of $\langle \Delta x^2 \rangle$ to the actual system size is central to the derivation of the classical diffusive equation (cf. Appendix B). More importantly, the value of the relevant transport length scale σ can be estimated from measurements in small systems, so that the results of transport analyses can then be directly translated to larger systems by a simple scaling argument. Indeed, the global confinement time is predicted to scale as:

$$\tau \sim \tau_D \sigma^{-2}. \tag{37}$$

Recall that σ is normalized to the system size, so that $\tau \sim L^2$.

However, in fusion plasmas it is observed that $\tau \sim L^\alpha$, with $\alpha < 2$ [8]. Within the diffusive framework, this result is often interpreted in the sense that $\langle \Delta x^2 \rangle$ (and thus D) appears to *increase* with system size [24]. However, from the point of view adopted in this paper, this result would rather appear to imply that there is *no* characteristic length scale, but instead, that all scales contribute, up to the cut-off imposed by the system size. In fact, this behaviour is obtained in a natural fashion within the CTRW model when the Gaussian step size pdf is replaced by Lévy stable distributions [25]. Such pdfs are characterized by four numbers (cf. Appendix A), the most relevant for this discussion being the so-called decay index, α ($0 < \alpha \leq 2$), describing the decay of the pdf which scales as $x^{-(\alpha+1)}$ for large x. All pdf moments of order $k > \alpha$ diverge (when $\alpha < 2$). Thus, most Lévy pdfs do not have a finite variance, and the calculation of $\langle \Delta x^2 \rangle$ along the lines of Eq. (36) leads to a result that increases with the system size (cf. Appendix D), in accordance with observation. This suggests that the use of Lévy stable distributions to describe transport might be a way to reproduce the experimentally observed scaling of the global confinement time.

However, as elaborated in detail in Appendix D, the appearance of Lévy pdfs in the description of transport, in combination with the finite size of the system, leads to a situation in which the transport coefficients (i.e. finite-size moments of the pdf) depend explicitly on the system size, even for small values of σ. Thus, such transport coefficients, measured in a system with a certain size, cannot be used to predict transport in a system with a different size. As mentioned in the introduction, at least two complementary approaches for describing transport characterized by Lévy pdfs are capable of handling this situation adequately: we may either replace the standard diffusive equation by a fractional differential equation (FDE) [26] or use the ME formalism. In this paper, we explore only the second possibility.

D. Power degradation

In this subsection, we will discuss under what conditions the CTRW model may exhibit *power degradation*. The effect of power degradation is observed experimentally in fusion plasmas as a dependence of the global confinement time on the external source rate in the form $\tau \sim S_{tot}^{-\gamma}$ ($\gamma > 0$) [8]. The model presented in Eq. (29) appears not to allow such

behaviour, since N_{tot} depends linearly on S_{tot} for any fixed choice of p. However, *a priori* there is no need to restrict the model to such a choice. In principle, either p or ψ may be chosen to depend on e.g. $n(x,t)$ or on any of its derivatives. However, one must be careful to avoid invalidating the derivation of Eq. (29). It turns out that Eq. (29) is still valid if the nonlinearities are restricted to a step size pdf of the form:

$$p(x-x',x';t) = p\left(x-x',x';t;f\left[n(x',t),\frac{dn}{dx}(x',t),...\right]\right). \tag{38}$$

which is why we initially assumed an explicit dependence on time and space of the joint pdf ξ. The interpretation of Eq. (38) is that, *at the time it performs a jump*, the walker takes the local values of the density and its derivatives into account to choose the length of the jump.

E. A minimal transport model

We now dispose of all the essential elements to build a tentative CTRW model with relevance for the systems under investigation. Naturally, the proposed "toy model" does not pretend to provide a complete description of transport in a real plasma. In particular, it describes just one field (say, the plasma density), while in fusion plasmas several other fields (such as the temperature) play a fundamental role. Even so, extensions to the model are rather straightforward to build, and this simplified model will be sufficient to demonstrate our main point: that it is possible to provide a satisfactory description of transport in a system that lacks characteristic length scales and exhibits power degradation.

For practical reasons, we want to be able to use a ME to describe the model. For simplicity, we will limit ourselves to CTRWs with an exponential waiting time distribution, so that steady state is easily accessible. We can achieve this by choosing a joint pdf ξ of the form:

$$\xi(x-x',x';t-t';t) = p\left(x-x',x';f\left[n(x',t),\frac{dn}{dx}(x',t),...\right]\right)\cdot\frac{e^{-(t-t')/\tau_D(x')}}{\tau_D(x')}, \tag{39}$$

as follows from the previous sections. The non-linearity in p is needed to obtain power degradation, and with proper functional dependencies introduces a certain degree of complexity

in the model, leading to very rich behavior, including fluctuations around a mean value and rapid propagation phenomena.

The associated ME is given by:

$$\frac{\partial n(x,t)}{\partial t} = S(x) - \frac{n(x,t)}{\tau_D(x)} + \int_0^1 dx' p\left(x - x', x'; f\left[n(x',t), \frac{dn}{dx}(x',t), ...\right]\right) \frac{n(x',t)}{\tau_D(x')}, \quad (40)$$

yielding a recursive equation for the steady state, time-independent particle density ($\partial n/\partial t = 0$):

$$n(x) = \tau_D(x)\left[S(x) + \int_0^1 dx' p\left(x - x', x'; f\left[n(x'), \frac{dn}{dx}(x'), ...\right]\right) \frac{n(x')}{\tau_D(x')}\right]. \quad (41)$$

Eqs. (40) and (41) are the most powerful tools in the CTRW framework. Note however that Eq. (41) may not converge, depending on the choice of f.

We obtain scale-free transport by using step size pdfs p that involve Lévy distributions, as described above. These prescriptions complete our CTRW model. Actual choices must now be made to address any problem of interest.

III. NUMERICAL STUDY

In this Section, we shall investigate a numerical toy model designed along the lines of the preceding Section. The system we have chosen is inspired on a common observation made in experiments with confined plasmas: the anomalous scaling of the global confinement appears to be related to the fact that some critical threshold is superseded [27]; here, we assume that this threshold is a critical density gradient, $(dn/dx)_c$. To model this behaviour, we choose p to be composed of two pdfs, one Gaussian ($\alpha = 2$) and another Cauchy ($\alpha = 1$), combined in such a way that the (slow) diffusive transport channel is active only when the local density gradient is less than the critical value, while the (fast) anomalous channel takes over control of the local transport when the threshold is overcome:

$$p\left(x - x'; \frac{dn}{dx}(x';t)\right) = \zeta(x',t)\ P_{sym}(x - x', 1, \sigma_1) + (1 - \zeta(x',t) P_{sym}(x - x', 2, \sigma_2) \quad (42)$$

The definition of P_{sym} is provided in Appendix A. Here we have defined

$$\zeta(x',t) = \Theta\left[\left|\frac{dn}{dx}(x',t)\right| - \left(\frac{dn}{dx}\right)_c\right]. \tag{43}$$

Since $\Theta(x)$ is the usual Heaviside step function, $\zeta(x',t)$ can be either one or zero, depending on the value of the local density gradient. The model is then completed, for simplicity, by assuming a spatially uniform waiting time pdf with constant mean waiting time τ_D, and a constant prescribed source rate profile, $S(x)$.

In the next sections, after giving a brief description of the numerical techniques used in Sec. III A and stressing the advantages of the ME approach in Sec. III B, we proceed to examine the system to look for signs of power degradation (Sec. III C) and non-diffusive scaling (Sec. III D) of the global confinement time. Finally, in Sec. III E we demostrate that the model exhibits superdiffusive propagation. With this example, we pretend to show the adequacy of the proposed framework to model systems in which these phenomena are observed, as is the case of confined plasmas.

A. Numerical implementation of the model

First, we have programmed the toy model in the form of a CTRW particle tracking code. Second, we have programmed a time evolution code according to the Master Equation (ME) corresponding to the same model as the chosen CTRW.

The CTRW model description is as follows: the one-dimensional space variable x covers the range $0 \leq x \leq 1$. Particles are added according to a preset constant fueling rate $S(x)$ (number of particles per time and space unit). Initially, the system time t is set to zero. A preset amount of particles is loaded to initialize the system. When a particle (i) is added (at a random position according to the distribution $S(x)$), it is assigned a waiting time τ_i (selected randomly from an exponential distribution with mean τ_D) after which it will perform a jump.

The iterative part of the program is as follows: The program searches for the first particle to jump next. Once found, particles are added according to the length of the time interval from the current time to the first jump time, matching the given fueling rate. Then the system is searched again for the first particle to jump and the system time is advanced to this time. This particle now performs a jump with a size drawn from a step distribution. If the particle jumps out of the spatial range, it is lost. If not, it is assigned a new waiting

time. Finally, the whole process is repeated iteratively.

In the realization presented here, we have chosen the waiting time $\tau_D = 1$ and set $S(x) =$ constant. To compute particle density profiles $n(x)$, it is necessary to divide the continuous space variable in discrete bins, and count the number of particles in each bin. We set the number of bins to 200. The gradient $dn/dx(x,t)$ is computed from the 5-points smoothed density profile $n(x)$, in order to reduce statistical fluctuations in this quantity. The particle step distribution for a jump from position x' to position x is given by Eq. (42) with $(dn/dx)_c = 50$, $\sigma_1 = 0.04$ and $\sigma_2 = 0.02$. Results are always evaluated after initial transients have died out (i.e. when the system has reached steady state).

The corresponding ME is Eq. (40) with $\tau_D(x) = 1$ and p given by Eq (42). To advance it in time, standard integration techniques for stiff differential equations are applied [28].

B. Convergence of the numerical CTRW model to the Master Equation

To study the effect of the number of particles in the CTRW model on the results, we have run the code with different fueling rates, while varying the critical gradient in proportion to the fueling rate. Thus, these runs are equivalent except for the number of particles N in the system. In Fig. 1, the results are compared to a run with the Master Equation, which corresponds to the limit $N \to \infty$.

The convergence of the CTRW results to the ME are clear, and the practical advantages of using the ME model are evident: (a) the CPU time consumption is much less than the CTRW model (when the number of particles is high) and (b) it corresponds much better to our physical system, namely a plasma with $\sim 10^{20}$ particles (such an amount of particles being impossible to simulate with the CTRW code, even on the fastest computers to date). The results presented in the following subsections have therefore been obtained by the ME code.

C. Scaling of the global confinement time with the external fueling

The toy model has two limits as a function of the external fueling S: at weak fuelling ($S < S_c$), the anomalous transport channel is never activated since the gradient remains below critical everywhere; while at very strong fueling ($S >> S_c$) the system behaves almost

as a purely anomalous system, with a super-critical gradient ($|dn/dx| > (dn/dx)_c$) almost everywhere. The core of the system (the region around $x = 1/2$) is an exception, because symmetry requires that the gradient is always zero in the center. Therefore, there remains always a (small) central region where transport is diffusive (not anomalous), even at very strong fueling. Characteristically, it shrinks in size as the fueling is increased but never vanishes.

In an intermediate situation, between weak and strong fueling, the system is divided into two main regions (cf. also **Refs. 29, 30**): a central region where transport is diffusive and a periphery where the gradient is critical (Fig. 2). In the central region, the slope of the profile can be computed, to good approximation, as (using Eq. (35) and symmetry):

$$\frac{dn}{dx} = -\left(\frac{S\tau_D}{\sigma_2^2}\right)(x - 1/2), \tag{44}$$

The crossing-over point between the two regions is the point where $|dn/dx| = (dn/dx)_c$:

$$\left|x_c - \tfrac{1}{2}\right| = \frac{\sigma_2^2}{S\tau_D}\left(\frac{dn}{dx}\right)_c = 0.02\ S^{-1} \tag{45}$$

with our parameter choices. So, the critical power threshold that must be overcome for the anomalous channel to become active is given by:

$$S_c = \frac{2\sigma_2^2}{\tau_D}\left(\frac{dn}{dx}\right)_c = 0.04. \tag{46}$$

Except for the pedestal contribution, the particle content of the system can easily be computed, since the gradients in both regions are known (the gradient in the periphery being critical *provided* the system is not over-driven, i.e. transport in the periphery is still characterized by a mixture of both transport channels, and not completely dominated by anomalous transport). Thus, we can integrate the curve sketched in Fig. 2 (ignoring the unknown pedestal) and find for the partial particle content (i.e. without the pedestal contribution):

$$N_{partial} = \begin{cases} \dfrac{S\tau_D}{12\sigma_2^2} & (S < S_c) \\[2ex] \dfrac{1}{4}\left(\dfrac{dn}{dx}\right)_c - \dfrac{\sigma_2^4}{3S^2\tau_D^2}\left(\dfrac{dn}{dx}\right)_c^3 & (S \geq S_c) \end{cases} \tag{47}$$

The confinement time can simply be evaluated from $\tau = N_{tot}/S_{tot}$ as before. Taking into account that the result must tend to the anomalous limit ($\tau \sim \tau_D/\sigma_1$) for large S, we find:

$$\tau_{partial} = \begin{cases} \dfrac{\tau_D}{12\sigma_2^2} & (S < S_c) \\ \max\left[\dfrac{1}{4S}\left(\dfrac{dn}{dx}\right)_c - \dfrac{\sigma_2^4}{3S^3\tau_D^2}\left(\dfrac{dn}{dx}\right)_c^3, \dfrac{c\tau_D}{\sigma_1}\right] & (S \geq S_c) \end{cases} \tag{48}$$

where c is a constant. This behavior is reflected by the scan of S presented in Fig. 3. Clearly, in the weak fueling limit the system confinement time scales as described in Appendix B (Eq. (B8), $\tau \propto \tau_D/\sigma^2$), while at strong fueling it scales as described in Appendix C ($\tau \propto \tau_D/\sigma$). In neither of these limiting cases does τ depend on the fueling S. But when the system becomes critical and a mixing of zones characterized by locally diffusive and anomalous transport occurs, a gradual transition between the two limiting cases takes place, which depends on the fraction of space occupied by the anomalous channel, and therefore on S.

Interesting is also the plot of the CPU time used per iteration (Fig. 4), since this is a direct measure of the complexity of the system: when the complexity is high, the sub-iteration time step is reduced accordingly, leading to an increase in overall CPU time consumption. The degree of complexity (or disorder) is related to the self-regulating character of this system state, and is particularly high just above the threshold, as is evident from the figure. It is associated with complex fluctuating behavior in both space and time.

D. Scaling of the confinement time with system size

The generic scaling behavior obtained in the previous section can also be used to understand the scaling of the confinement time with system size. Since we have normalized the system size to $L = 1$, a scaling of the system size is equivalent to a scaling of σ. The constant c appearing in Eq. (48) can be estimated numerically for our system and we find $c = 0.45$. In Fig. 5, we have plotted $\tau_{partial}$ as a function of σ_2 and S (with $\sigma_1 = 2\sigma_2$). At each choice of σ_2, the system behaves as in the previous section: at low S, the system is fully diffusive (Gaussian); at high S, the system is completely anomalous; and in-between, the system is critical. In the critical situation, the confinement time is determined almost

exclusively by the fueling S and the critical gradient $(dn/dx)_c$; the waiting time τ_D and the step size σ_2 do not play any significant role – or, in other words, they do not act as the characteristic scales of the transport.

E. Rapid transport phenomena

The model produces rapid transport phenomena, which bear a remarkable similarity to the rapid phenomena observed in fusion experiments [31–35]. To demonstrate this effect, we have taken the ME simulation corresponding to $S = 0.2$ in Section III C. For $t < t_{cp} = 1001$, the system is in steady state. We induce an artificial "cold pulse" by setting $n(x, t_{cp}) = 0$ for $x \geq 0.875$. Then we follow the evolution of the system. Fig. 5 shows the time development of $n(x, t)$. The cold pulse and its effects are clearly seen. The pulse creates an inward-propagating "cold" front (i.e. with reduced density). Fig. 6 shows the same data, however after subtracting the steady state profile in order to stress the perturbation. The "cold" front reaches the center of the system ($x = 0.5$) in about $\Delta t = 0.1$. This number should be compared to the confinement time for the system (cf. Fig. 3): $\tau = 70$. Thus, the front propagates nearly three orders of magnitude faster than might be expected from the global confinement time! Note that the propagation is "ballistic" in the sense that it does not slow down as it propagates, as would be expected for diffusive propagation (cf. **Ref. 36** for experimental observations of this effect in fusion plasmas). The propagation velocity is related to the self-regulation mechanism of the system, which activates or deactivates the rapid transport channel in order to maintain the gradient close to critical.

IV. DISCUSSION

As stated in the introduction, transport in fusion plasmas is exceedingly complex. Apart from classical diffusion driven by collisions [37], many other mechanisms are known that contribute to plasma transport. In this respect, we could mention neoclassical transport [2, 38], transport associated with stochastic magnetic fields [5, 6] and transport driven by turbulence, associated with rational surfaces or zones with strong gradients [3, 4]. There is good evidence that most of these **physical mechanisms may yield** contributions to transport **that** are non-Fickian [1, 39, 40]. **Recent tracer-particle simulations of resis-**

tive pressure-gradient-driven turbulence suggest that the radial excursion of the tracer-particles scale with time as:

$$< x^2 >^{1/2} \sim t^{0.88}, \tag{49}$$

i.e. much higher than the value of 0.5 than is to be expected from diffusive transport [16]. A similar value for this exponent has also been obtained in experiment, from the analysis of density fluctuations measured at the edge of the DIII-D tokamak [15].

The main difference between the mentioned simulations and more standard turbulence simulations is that, in the former, equilibrium profiles are evolved in time and the system is driven weakly. In this situation, the local eddies that are excited when an instability threshold is surpassed can dispose efficiently of the free energy excess and disappear after bringing the profile back below marginality – i.e. the eddies are allowed to affect the background profile. In this situation, the spatio-temporal dynamics of the simulation self-regulate, generating "emergent" behavior.

It is suggested that the cause for the appearance of Lévy distributions in transport must be sought in the existence such a self-regulation mechanism. The appearance of this mechanism requires the existence of an effective competition between the time scales associated with the driving rate and the local energy redistribution rate. This state of things may indeed be present at certain stages in a confined plasma (L mode). For this reason, it seems reasonable to expect that transport in fusion plasmas may be better described by **evolution** equations that are not limited to Fickian (classical diffusive) transport [36].

In the present paper we propose a general framework to explore this conjecture, that might provide a first step towards reaching a satisfactory description of these phenomena in the near future. The non-Fickian transport **channel** is modeled by means of a particle step pdf that takes the form of a Lévy distribution. But, at the same time, it accomodates the important phenomenon of "power degradation" within the description by means of a non-linear modification of the step pdf, rather similar to the way this issue is handled in the standard Fickian transport framework [32]. In contrast to the latter, however, the present description permits the extrapolation of transport properties to larger systems, since the

relevant quantities (i.e., α, σ, etc.) are independent of the system size (cf. Appendix D).

We have also built a 'toy model' that incorporates all these ingredients and that, as a result, exhibits anomalous transport and power degradation. The resulting feedback mechanism also leads to "stiff" profiles, reminiscent of the phenomenon of "profile consistency" [41] encountered in confined plasmas. The main physical element used to construct the toy model, namely a critical gradient that switches dominance of transport between a Fickian and a non-Fickian **channel**, is inspired by the phenomenology observed in fusion experiments. Indeed, the theory of plasma instabilities learns us that manifold instabilities are triggered when local gradient thresholds are overcome. Such is the case for all pressure-driven modes. The fast non-Fickian transport **channel**, activated when the gradients exceed a threshold value, is suggested by turbulence simulations that show that the effectiveness of turbulence to drive transport depends strongly on the departure of the gradient above the critical gradient. Thus, transport is discontinuous through this limit, or at least strongly non-linear.

We believe that the proposed approach might also be the best framework to explore the relevance of the ideas of self-organized criticality (SOC) to plasma transport, as claimed by several authors [18, 20]. Most of these studies were limited, by necessity, to drawing analogies between plasma transport and sandpile models [19, 30, 42]. This limitation might be removed by considering the current modelling framework. An investigation into the self-organizing properties of this model is currently underway, and a detailed analysis of these issues will be the subject of a future paper.

One final issue needs to be mentioned before attempting to construct a transport code based on these ideas. As said before, our 'toy model' assumes, for reasons of simplicity, an exponential distribution for the waiting time pdfs of the walkers. However, some recent estimations, obtained from experimental measurement and the modelling of turbulence suggest that a Lévy waiting-time pdf (with $\alpha \simeq 0.8$ [15, 16]) might correspond better to what is observed. A careful analysis of this issue must therefore be undertaken prior to the construction of a CTRW model for transport in the corresponding plasmas.

V. CONCLUSIONS

In summary, we have proposed a model, well-anchored in theoretical and experimental results, that may provide a path towards a unified transport framework for describing the experimental phenomenology of global transport. It is based on simple physical principles, viz. a (non-linear) generalization of Brownian motion to Lévy probability distributions. In spite of their conceptual simplicity, the underlying physical principles considered represent a significant philosophical departure from the standard Fickian transport paradigm, dominant in the analysis of transport in fusion plasmas up to date, although the model presented contains Fickian transport as a special case.

We believe that this kind of approach (either in the form of a Master Equation, as in this paper, or by means of some other equivalent formalism) may lead to the construction of a full-blown transport code that might provide a better understanding of the remarkable scaling properties of fusion plasmas. Indeed, the simple model examined in this paper already shows that capturing this complicated phenomenology within such a framework appears to be possible. Extensions involving several coupled fields, with a number of probability distribution functions (either derived from microscopic transport theory or measured directly from the experiment) for modelling the relevant microscopic transport mechanisms, might also be considered.

Finally, we remark that the modeling framework proposed here is quite ample and may find applications in fields other than fusion research, such as spatio-temporal chaos, fluid turbulence, chemical reaction-diffusion problems, etc.

APPENDIX A: LÉVY DISTRIBUTIONS

A random variable that is the sum of N independent identically distributed (i.i.d.) random variables is distributed according to a Lévy distribution in the limit of large N (Theorem due to Khintchine and Lévy, proof by Gnedenko and Kolmogorov [43]). When the first and second statistical moments (the mean and variance) of the i.i.d. variables are finite, then the limit distribution of their sum is a particular Lévy distribution known as the Gaussian distribution, which explains the ubiquity of the latter in nature. Yet non-Gaussian Lévy distributions have been observed in many processes in different branches of science (cf. **Ref. 13**

and references therein); the interest of non-Gaussian Lévy distribution lies here in the fact that the random walk associated to such distributions is very different from the ordinary random walk (Brownian motion), and leads to anomalous diffusion [12].

No explicit expression for the Lévy distributions exists, but their characteristic function is [25]:

$$P(k) = \begin{cases} \exp\left[-\sigma^\alpha |k|^\alpha \left(1 - i\beta \frac{k}{|k|} \tan\left(\frac{\pi\alpha}{2}\right)\right) + i\mu k\right], & \alpha \neq 1 \\ \exp\left[-\sigma |k| \left(1 + i\beta \frac{2k}{\pi|k|} \ln|k|\right) + i\mu k\right], & \alpha = 1 \end{cases} \tag{A1}$$

The Lévy distributions are characterized by 4 parameters: their mean ($-\infty < \mu < \infty$), their scale or width ($0 \leq \sigma < \infty$), their skewness ($-1 \leq \beta \leq 1$) and their stability or decay index ($0 < \alpha \leq 2$). The distribution $P(x)$ can be found numerically, with any required precision, by taking the inverse Fourier transform of a discrete representation of Eq. (A1).

The symmetric α-stable Lévy distributions referred to in this paper are a subclass of Eq. (A1), defined by $\mu = \beta = 0$. We define

$$P_{sym}(x, \alpha, \sigma) = \int P(k)|_{\mu=\beta=0} \exp[ikx]\, dk \tag{A2}$$

The symmetric α-stable distribution with $\alpha = 2$ and scale σ is equal to a Gaussian with width $w = \sqrt{2}\sigma : P(x) = exp[-x^2/(4\sigma^2)]/[2\sigma\sqrt{\pi}]$. The symmetric α-stable distribution with $\alpha = 1$ and scale σ is equal to a Cauchy distribution with width $\sigma : P(x) = \sigma/[\pi(\sigma^2 + x^2)]$.

A sequence of random numbers corresponding to the distributions Eq. (A2) can be generated efficiently using the technique described in [44]; namely, by computing the sum of independent random variables with the correct distribution of the "tail", which converges automatically to the required Lévy distribution.

APPENDIX B: STEADY STATE WITH STEP-SIZE PDF WITH FINITE VARIANCE

We wish to study the behavior of the confinement time τ for a step size pdf $p(x - x', x')$, and with $\tau_x = \tau_D$ and $S(x, t) = S(x)$. Eq. (29) becomes:

$$\frac{\partial n(x,t)}{\partial t} = \frac{1}{\tau_D}\left[\int_0^1 n(x',t)p(x-x',x')dx' - n(x,t)\right] + S(x) \tag{B1}$$

We will use a Tailor expansion for $n(x', t)$, defining $x' = x - \Delta x$:

$$n(x',t) = n(x-\Delta x,t) = n(x,t) - \Delta x\frac{\partial n}{\partial x} + \frac{\Delta x^2}{2}\frac{\partial^2 n}{\partial x^2} - ... \tag{B2}$$

Next, we assume that $p(x-x',x') = p(\Delta x,x')$ is a narrow function, peaking at $\Delta x = 0$, satisfying

$$\begin{aligned} \int_{-\infty}^{\infty} p(\Delta x, x-\Delta x)d\Delta x &= 1 \\ \int_{-\infty}^{\infty} \Delta x p(\Delta x, x-\Delta x)d\Delta x &= 0 \\ \int_{-\infty}^{\infty} \Delta x^2 p(\Delta x, x-\Delta x)d\Delta x &= 2\sigma^2 \end{aligned} \tag{B3}$$

If $\sigma \ll x \ll 1-\sigma$ (and therefore also $\sigma \ll 1$), the integration limits in Eq. (B1) can be extended to infinity and we obtain, after substituting Eq. (B2) into Eq. (B1) and using Eq. (B3):

$$\frac{\partial n}{\partial t} = \frac{\sigma^2}{\tau_D}\frac{\partial^2 n}{\partial x^2} + S \equiv D\frac{\partial^2 n}{\partial x^2} + S \tag{B4}$$

which is the standard (Fickian) diffusion equation, valid in most of the region $0 \leq x \leq 1$, except near the boundaries (due to the failure of the approximation involving the infinite limits in Eqs. (B3)), and for all p's satisfying Eqs. (B3). An additional convection term is obtained if the second requirement of Eq. (B3) is relaxed. According to the Central Limit Theorem, any PDF satisfying Eq. (B3) will converge to a Gaussian shape when many individual steps of the particles in the system are summed [45].

Thus we find that the standard diffusion result is recovered in this approximation. The corresponding static solution ($\partial n/\partial t = 0$) can be found from Eq. (B1):

$$n(x) \approx \int_{-\infty}^{\infty} n(x')p(x-x',x')dx' + S(x)\tau_D \tag{B5}$$

where we have extended the integration limits to infinity for simplicity. This equation permits finding easy approximate analytical solutions in concrete cases. Eq. (B5) determines $n(x)$ up to a constant if we impose symmetry ($n(x) = n(1-x)$). To find this constant, one must impose particle balance:

$$\Gamma(1) - \Gamma(0) = \int_1^\infty \int_0^1 n(x')p(x-x',x')dx'dx + \int_{-\infty}^0 \int_0^1 n(x')p(x-x',x')dx'dx = S_{tot} \tag{B6}$$

By way of example, assume the step distribution is a Gaussian, $p(x-x',x') = p(x-x')$, with width $w = \sqrt{2}\sigma$:

$$p(\Delta x) = \frac{\exp\left[-\Delta x^2/\left(4\sigma^2\right)\right]}{2\sigma\sqrt{\pi}} \tag{B7}$$

For $S(x) = S_0$, we expand $n(x) = n_0 + n_1 x(1-x)$ (ignoring higher order terms), solve for n_1 using Eq. (B5), and then evaluate τ using Eq. (33). For simplicity, the constant n_0 is not evaluated, although it might be found using Eq. (B6). We find:

$$\tau = \frac{\tau_D}{12\sigma^2} + \frac{n_0}{S_{tot}} \tag{B8}$$

For $S(x) = 6S_0 x(1-x)$, we expand $n(x) = n_0 + n_1 x(1-x) + n_2 x^2(1-x)^2$, solve for n_1 and n_2 using Eq. (B5) and find:

$$\tau = \tau_D\left(\frac{1}{10\sigma^2} + \frac{1}{2}\right) + \frac{n_0}{S_{tot}} \tag{B9}$$

In these expressions, only the leading term (usually dominant for σ small) is due to transport inside the system; but additionally, there is a term (n_0/S_0) that depends only on σ (it does not depend on either τ_D or S), which is associated with the density pedestal n_0 due to the finite size of the system.

APPENDIX C: STEADY STATE WITH AN α-STABLE LÉVY DISTRIBUTION

When the step probability distribution is a symmetric α-stable Lévy distribution with zero mean, its Fourier transform is given by (cf. Appendix A).

$$p(k) = exp(-\sigma^\alpha |k|^\alpha) \tag{C1}$$

First, we study the static solution, given by Eq. (B5) in the limit of small σ, repeated here for convenience:

$$n(x) \approx \int_{-\infty}^{\infty} n(x')p(x-x')dx' + S(x)\tau_D \tag{C2}$$

Further on we will discuss the consequences of finite σ. Eq. (C2) can be Fourier transformed to yield:

$$n(k) = n(k)p(k) + S(k)\tau_D \tag{C3}$$

or:

$$n(k) = \frac{S(k)\tau_D}{1 - p(k)} \tag{C4}$$

Fourier-inverting Eq. (C4) yields:

$$n(x) = \frac{\tau_D}{2\pi} \int_{-\infty}^{\infty} \frac{S(k)}{(1 - e^{-\sigma^\alpha |k|^\alpha})} e^{ikx} dk \tag{C5}$$

Since σ is assumed to be small and $\alpha > 0$, $1 - e^{-\sigma^\alpha |k|^\alpha} \approx \sigma^\alpha |k|^\alpha$, so that:

$$n(x) \approx \frac{S_0 \tau_D}{\sigma^\alpha} f(x) \tag{C6}$$

where we have used $S(x) = S_0 s(x)$ with $\int s(x)dx = 1$. This leads to the confinement scaling $\tau \propto \tau_D/\sigma^\alpha$ (cf. Fig. 8).

As an example, we take $S(x) = S_0(\Theta(x) - \Theta(x-1))$, where $\Theta(x)$ is the Heaviside function. Then $S(k) = iS_0(e^{-ik} - 1)/k$ and

$$n(x) \approx \frac{S_0 \tau_D}{2\pi\sigma^\alpha} \int_{-\infty}^{\infty} \frac{i|k|^{-\alpha}}{k} (e^{-ik} - 1) e^{ikx} dk \tag{C7}$$

This integral diverges in general. However, its Cauchy Principal Value is:

$$n(x) \approx -\frac{S_0 \tau_D}{\pi\sigma^\alpha} \Gamma(-\alpha) sin\left(\frac{\alpha\pi}{2}\right) [x^\alpha + (1-x)^\alpha] \tag{C8}$$

(only valid for $0 \leq x \leq 1$ and non-integer positive values of α).

APPENDIX D: SCALING BREAKDOWN OF THE DIFFUSIVE APPROACH WITH α-STABLE LÉVY DISTRIBUTIONS

The validity of the approximation Eq. (B5), used in Appendix C, is however questionable for finite σ, in particular when the step probability distribution is a Lévy distribution, since the mean and standard deviation of the step size may diverge. Then, the presence of the

system boundaries is "felt" throughout the system, in contrast to the Gaussian case, where the presence of the system boundaries may be neglected for small but finite σ. This effect leads to additional "diffusive" and "convective" terms in the approximate diffusive equation corresponding to the system, which are exclusively due to boundary effects. To see this, we rewrite Eq. (B3), now explicitly taking account of the finite system size:

$$\begin{aligned} \int_0^1 p(x-x',x')dx' &= \mu_0(x,\alpha,\sigma) \\ \int_0^1 (x-x')p(x-x',x')dx' &= \mu_1(x,\alpha,\sigma) \\ \int_0^1 (x-x')^2 p(x-x',x')dx' &= \mu_2(x,\alpha,\sigma) \end{aligned} \tag{D1}$$

We can still use the Taylor expansion of Eq. (B2) with $\Delta x = x - x'$, but now we find:

$$\frac{\partial n}{\partial t} \approx \frac{1}{\tau_D}\left[(\mu_0(x,\alpha,\sigma)-1)n - \mu_1(x,\alpha,\sigma)\frac{\partial n}{\partial x} + \frac{\mu_2(x,\alpha,\sigma)}{2}\frac{\partial^2 n}{\partial x^2}\right] + S(x) \tag{D2}$$

where $\mu_0(x,\alpha,\sigma) < 1$, so that the first term on the right-hand side of Eq. (D2) represents a direct particle loss term due to the finite system size. Note that in the case that $p(\Delta x, x') = f(\Delta x)$ and $f(-\Delta x) = f(\Delta x)$, we deduce from Eq. (D1) that $\mu_1(x,\alpha,\sigma)$ has the same sign as $(x - 1/2)$, so typically $\mu_1(x,\alpha,\sigma)\partial n/\partial x \leq 0$ for all x (outward convection). Inward convection can be obtained when $p(\Delta x, x')$ depends on x' or when p is not symmetric.

Thus, the finite size of the system combined with step distributions of the Lévy type leads to a diffusion equation that includes direct loss terms and convection terms. However, it is perhaps not generally realised that in this case, the coefficients appearing in the diffusion equation Eq. (D2) depend explicitly on the parameters of the distribution (here, α and σ). Since σ is the width of the step distribution, normalized to the system size, this means that, in general, the coefficients μ_i appearing in the diffusion equation depend on the system size. This effect is shown graphically in Fig. 9. In other words, when a given experiment is modelled by an equation of the type Eq. (D2), the coefficients that are thus obtained cannot be used to predict what would happen in a similar system of e.g. twice the size of the system studied! The pdf itself, however, does allow scaling and determining the pdf of transport therefore provides a valid method to make scaling predictions.

[1] R. Balescu, Phys. Rev. E 51, 4807 (1995)

[2] F.L. Hinton and R.D. Hazeltine, Rev. Mod. Phys. 48, 239 (1976)

[3] P.C. Liewer, Nucl. Fusion 25, 543 (1986)

[4] A.J. Wootton, H.Y.W. Tsui and S. Prager, Plasma Phys. Control. Fusion 34, 2023 (1992)

[5] G. M. Zaslavsky, R. Z. Sagdeev, D. A. Usikov and A. A. Chernikov, Weak Chaos and Quasi-Regular Patterns, Cambridge University Press (1991)

[6] Y. Elskens and D. Escande, Microscopic Dynamics of Plasmas and Chaos, in Series in Plasma Physics, IOP Publishing Ltd. (2003) ISBN 0 7503 0612 2

[7] J.H. Misguich, J.-D. Reuss, D. Constantinescu, *et al.*, Plasma Phys. Control. Fusion 44, L29 (2002)

[8] B.A. Carreras, IEEE Trans. on Plasma Science 25 (6), 1281 (1997)

[9] K.W. Gentle, R.V. Braveneck, G. Cima, *et al*, Physics of Plasmas 2, 2292 (1995)

[10] E.W. Montroll, J. Math. Phys. 6 (2), 167 (1965)

[11] J. Klafter and R. Silbey, Phys. Rev. Lett. 44 (2), 55 (1980)

[12] J. Klafter, A. Blumen and M.F. Shlesinger, Phys. Rev. A 35 (7), 3081 (1987)

[13] R. Metzler, J. Klafter, Physics Reports 339, 1 (2000)

[14] G.M. Zaslavsky, Phys. Rep. 371, 461 (2002)

[15] G.M. Zaslavsky, M. Edelman, H. Weitzner, *et al*, Physics of Plasmas 7, 3691 (2000)

[16] B.A. Carreras, V.E. Lynch and G.M. Zaslavsky, Physics of Plasmas 8, 5096 (2001)

[17] P. Bak, C. Tang, and K. Wiesenfeld, Phys. Rev. Lett. 59, 381 (1987)

[18] P.H. Diamond and T.S. Hahm, Phys. Plasmas 2, 3640 (1995)

[19] D. Newman, B.A. Carreras, P.H. Diamond and T.S. Hahm, Phys. Plasmas 3 (8), 1868 (1996)

[20] B.A. Carreras, D. Newman, V.E. Lynch, and P.H. Diamond, Phys. Plasmas 3 (8), 2903 (1996)

[21] E.W. Montroll and M.F. Schlesinger, in Studies in Statistical Mechanics Ed. J.L. Lebowitz and E.W. Montroll (North-Holland, Amsterdam, 1984), Vol. 11, p.5

[22] N.G. van Kampen, Stochastic Processes in Physics and Chemistry (North-Holland, New York, 1981) ISBN 0-444-89349-0

[23] W.J. Shugard and H. Reiss, J. of Chem. Phys. 65 (7), 2827 (1976)

[24] Z. Lin, S. Ethier, T. S. Hahm, and W. M. Tang, Phys. Rev. Lett. 88, 195004 (2002)

[25] G. Samorodnitsky and M.S. Taqqu, Stable non-Gaussian processes (Chapman & Hall, New York, 1994) ISBN 0-412-05171-0

[26] R. Metzler, The European Physical Journal B, 19 (2), 249 (2001)

[27] D.R. Baker, C.M. Greenfield, K.H. Burrell *et al*, Phys. Plasmas 8, 4128 (2001)

[28] NAG Fortran Library Manual, Mark 18 (The Numerical Algorithms Group Ltd., 1997) ISBN 1-85206-147-2

[29] R. Sánchez, D.E. Newman, B.A. Carreras, Nucl. Fusion 41, 247 (2001)

[30] R. Sánchez, D.E. Newman, B.A. Carreras, R.A. Woodard, W. Ferenbaugh and H.R. Hicks, Nucl. Fusion 43, 1031 (2003)

[31] JET Team, Plasma Physics and Controlled Nuclear Fusion Research, 1994 (Proc. 15th Int. Conf. Plasma Physics and Nuclear Fusion Research, Seville, 1994), Vol. 1, IAEA, Vienna, p. 307

[32] K.W. Gentle, R.V. Bravenec, G. Cima, *et al.*, Phys. Plasmas 4, 3599 (1997)

[33] J.G. Cordey, D.G. Muir, S.V. Neudachin, *et al.*, Nucl. Fusion 35, 101 (1995)

[34] E.D. Fredrickson, K. McGuire, A. Cavallo, *et al.*, Phys. Rev. Lett. 65, 2869 (1990)

[35] M.W. Kissick, J.D. Callen, and E.D. Fredrickson, Nucl. Fusion 38, 821 (1998)

[36] B.Ph. van Milligen, Nucl. Fusion 42, 787 (2002)

[37] S.I. Braginskii, Transport in Plasmas, in Review of Plasma Physics, M.A. Leontovich (Ed. New York: Consultants Bureau, 1965, vol. 1) 205

[38] S. P. Hirshman and D. Sigmar, Nuclear Fusion 21, 1079 (1981)

[39] B.A. Carreras, B. van Milligen, C. Hidalgo, *et al.*, Phys. Rev. Lett. 83, 3653 (1999)

[40] V. Tribaldos, in Contr. Fusion and Plasma Phys. (Proc. 30th EPS Conf., St. Petersburg, 2003), ECA Vol. 27A, European Physical Society, P-1.19 (2003)

[41] ITER Group, Nucl. Fusion 39 (12), 2175 (1999)

[42] S.C. Chapman, R.O. Dendy and B. Hnat, Phys. Rev. Lett. 86, 2814 (2001)

[43] B.V. Gnedenko and A.N. Kolmogorov, Limit distributions for sums of indepen-

dent random variables, Addison Wesley, Reading, MA (1954)

[44] **A. V. Chechkin and V. Yu. Gonchar, A Model for Ordinary Levy Motion, Preprint lanl/gov cond-mat 9901064**

[45] **H. Stark, J. Woods, Probability, random processes and estimation theory for engineers (Prentice-Hall, Upper Saddle River, NJ, 1986), pp. 143-144**

FIGURE CAPTIONS

Fig. 1 – Steady state profiles of $n(x,t)$ after the initial transient phase has died out. It is seen how the CTRW model converges to the ME results (with $S = 0.5$) as the number of particles in the system is increased.

Fig. 2 – Sketch of the transport regions in the model, in a critical situation.

Fig. 3 – Confinement time as a function of the fueling rate S. The points are results from program runs, the continuous line is the theoretical relationship (which does not take account of the pedestal) derived in the text. Below $S = S_c = 0.04$ the system is sub-critical and the confinement time does not depend on S. At low and intermediate values of S, the theoretical line agrees well with the experimental points, although there is a small difference, caused by the pedestal. Finally, at the highest values of S criticality is lost in the periphery (the system is overdriven) and the experimental points tend asymptotically to the anomalous scaling limit (for which $\tau \approx 11.24$).

Fig. 4 – CPU time per iteration as a function of the fueling rate S. Upon crossing the critical threshold (at $S = 0.04$), there is a very important increase in CPU time consumption (by 3 orders of magnitude), reflecting the fact that the stiffness is strongly increased directly above the transition from sub-critical to critical. Above the threshold, there is a gradual decrease of CPU time as S increases, since increasing S implies a reduction in the relative importance of the stiffness-producing term involving the step pdf p in Eq. (29), so the integration routine can advance more rapidly (the expected scaling relation $t_{CPU} \propto 1/S$ is indicated in the figure). Another equivalent way of interpreting this graph is to consider the CPU time to be proportional to the spatial disorder of the system.

Fig. 5 – Scan of σ_2 and S, using Eq. (48).

Fig. 6 – Graph of $n(x,t)$. Cold pulse induced at $t_{cp} = 1001$.

Fig. 7 – Graph of $n(x,t) - \langle n(x,t) \rangle$. Cold pulse induced at $t_{cp} = 1001$.

Fig. 8 – In this plot, two step pdfs are compared. One is a Gaussian distribution with $\alpha = 2$ and $\sigma = 0.01/\sqrt{2}$ (i.e. with a standard deviation of 0.01, cf. Appendix A). The second is a Lévy or Cauchy distribution with $\alpha = 1$ and $\sigma = 0.01$. The Gaussian distribution has been divided by a factor 1.8 to emphasize the similarity of the central part of the distribution. The apparently unimportant difference in the tails of these distributions has the remarkable effect that the global confinement time, obtained after solving the transport equations as in

Appendix C (with $\tau_D = 1$ and $S(x) = 1$), differs by more than a factor 40.

Fig. 9 – Scaling of the finite-size moments $\mu_i(x, \alpha, \sigma)$, $i = 0, ..., 2$ of the step pdf, according to Eq. (D2), for step pdfs with $\alpha = 1$ and $\alpha = 2$, at $x = 0.75$ (i.e. halfway between the center and the edge of the system). The moments become independent on σ for small σ in the case $\alpha = 2$, whereas the moments always depend on σ in the case $\alpha = 1$. The implication of this is that transport coefficients (moments) obtained in systems of a given size (σ) cannot be extrapolated to systems of another size when the step distribution is not Gaussian ($\alpha = 2$).

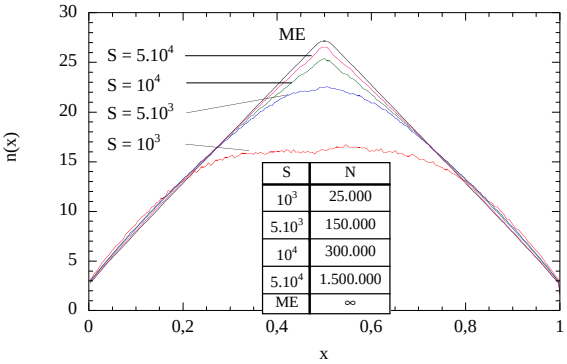
ME
S = 5.10^4
S = 10^4
S = 5.10^3
S = 10^3
n(x)
x
0
5
10
15
20
25
30
0
0,2
0,4
0,6
0,8
1
S | N
10^3 | 25.000
5.10^3 | 150.000
10^4 | 300.000
5.10^4 | 1.500.000
ME | ∞

FIG. 1:

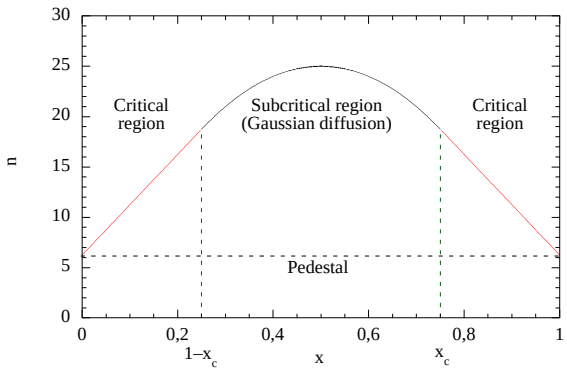
30
25
20
15
10
5
0
n
Critical
region
Subcritical region
(Gaussian diffusion)
Critical
region
Pedestal
0
0,2
0,4
0,6
0,8
1
1–x_c
x
x_c

FIG. 2:

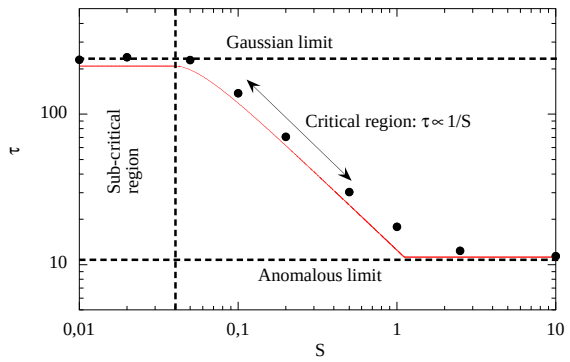
Gaussian limit
Critical region: τ∝ 1/S
Sub-critical region
Anomalous limit
τ
100
10
0,01
0,1
1
10
S

FIG. 3:

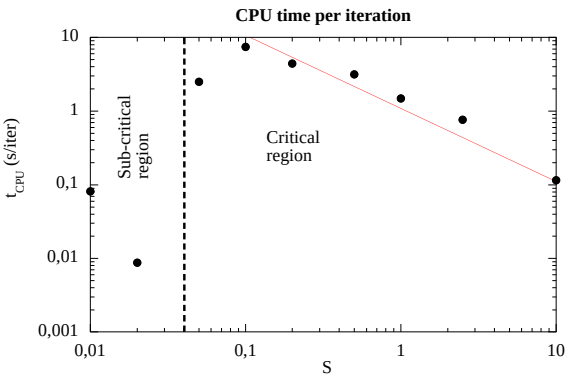
CPU time per iteration
10
1
0,1
0,01
0,001
0,01
0,1
1
10
S
t_{CPU} (s/iter)
Sub-critical region
Critical region

FIG. 4:

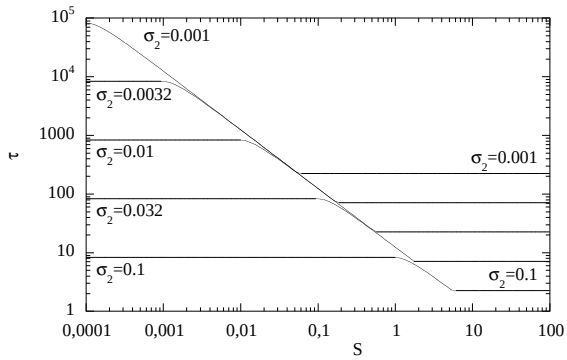
10^5
10^4
1000
100
10
1
τ
0,0001
0,001
0,01
0,1
1
10
100
S
σ_2=0.001
σ_2=0.0032
σ_2=0.01
σ_2=0.032
σ_2=0.1
σ_2=0.001
σ_2=0.1

FIG. 5:

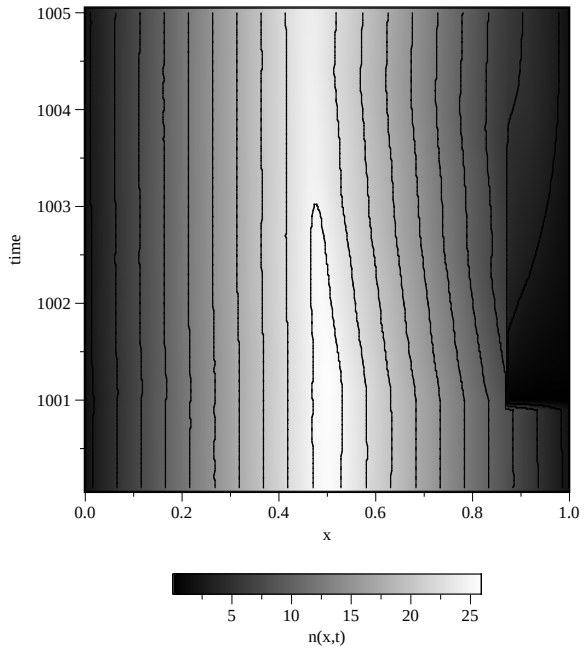

FIG. 6:

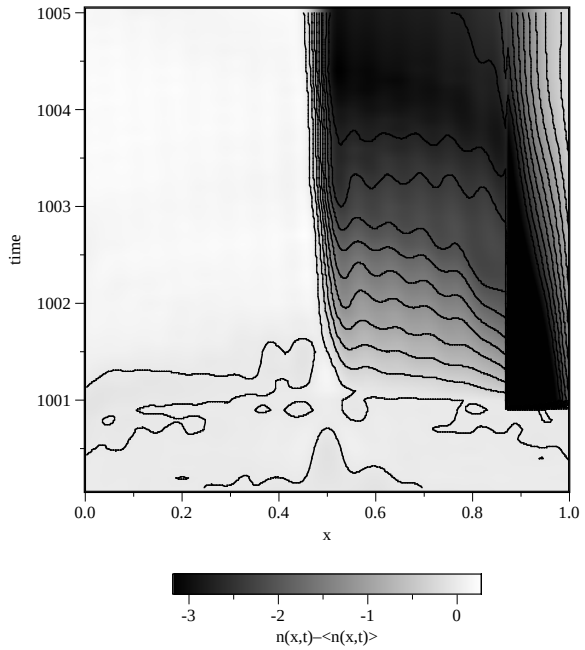

FIG. 7:

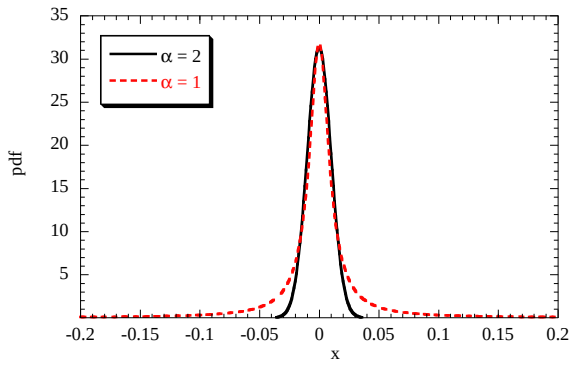

FIG. 8:

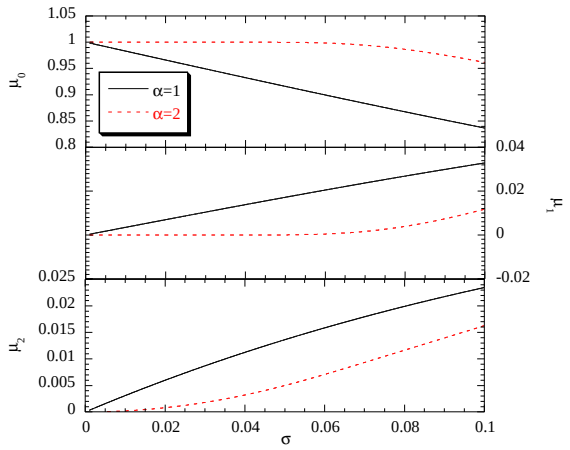
1.05
1
0.95
0.9
0.85
0.8
μ0
α=1
α=2
0.04
0.02
0
-0.02
μ1
0.025
0.02
0.015
0.01
0.005
0
μ2
0
0.02
0.04
0.06
0.08
0.1
σ

FIG. 9: